IEEE Access
Multidisciplinary ⋮ Rapid Review ⋮ Open Access Journal

Received January 4, 2022, accepted January 25, 2022, date of publication February 4, 2022, date of current version February 11, 2022.

Digital Object Identifier 10.1109/ACCESS.2022.3149042

An Improved Sliding Mode Direct Power Control Strategy Based on Reactive Power Compensation for Vienna Rectifier

YAODONG WANG[1,2], YINGHUI LI[1], AND SHUN HUANG[1,2]
[1]Aviation Engineering School, Air Force Engineering University, Xi'an 710038, China
[2]Graduate School, Air Force Engineering University, Xi'an 710038, China

Corresponding author: Yaodong Wang (1320996166@qq.com)

This work was supported in part by the Foundation of Air Force Engineering University Graduate Innovation Practice under Grant CXJ20211027.

ABSTRACT Vienna rectifiers are widely used in electric vehicle charging systems, wind power generation systems and other fields due to their excellent high-voltage resistance, small size and high efficiency. Aiming at the problems of the Vienna rectifier's long response time, low anti-disturbance ability, and current zero-crossing distortion, a new sliding mode direct power control strategy based on disturbance compensation is proposed. Firstly, a model considering the uncertainty is established, and the neural network is used to estimate and compensate the uncertain disturbance. Secondly, aiming at the slow approach speed and slow system convergence of traditional control methods, a new approaching law sliding mode direct power control strategy is designed. Aiming at the current zero-crossing distortion, the reason is analyzed and a compensation method is proposed. Finally, simulations and experiments show that the proposed method has no voltage overshoot and converges faster, effectively improving the problem of different phases of voltage and current. The rectifier operates at unit power, has better steady-state performance and stronger anti-load disturbance ability. The current total harmonic distortion is controlled below 2%, and the current quality is effectively improved.

INDEX TERMS RBF neural network, sliding mode control, uncertain model, Vienna rectifier.

I. INTRODUCTION

The current energy shortage has become a global problem, and the power supply is insufficient while the demand for electricity continues to increase [1], [2]. In this case, it is of great significance to improve the efficiency, power quality and anti-load disturbance ability of power conversion equipment [3], [4]. Vienna rectifier is a complex nonlinear system with multivariables, strong nonlinearity [5], [6] and high degree of coupling. Compared with the traditional two-level rectifier, the three-level Vienna rectifier has higher power factor, lower input current harmonic distortion, fewer switching devices, low voltage stress, and no breakdown phenomenon [7], [8]. It is widely used in uninterruptible power supplies (UPS), Wind power generation system [9], [10], new energy vehicle charging pile [11], [12], aviation power supply system.

The associate editor coordinating the review of this manuscript and approving it for publication was Guillaume Parent.

Although the Vienna rectifier has many advantages, it also has problems such as distortion of the grid-side current at the zero crossing [13]–[15], low robustness [16]–[18], high harmonic [19]–[23], content of AC current measurement, and low anti-load sudden loading/unloading ability [24]–[26]. In recent years, researchers have carried out a lot of research on the control strategy of Vienna rectifier.

Literature [27] combines finite control set model predictive control (FCS-MPC) with space vector modulation (SVPWM). The switching frequency is controlled by adjusting the carrier frequency, which reduces the harmonic content and improves the steady-state response time. The output voltage fluctuates greatly when switching loads.Literature [28] proposed a Vienna rectifier model predictive control strategy based on discrete space vector modulation (DSVM-MPC) to introduce virtual vectors to form a larger number of vector finite control sets to reduce the predicted voltage error and improve the quality of the input current waveform. But this algorithm is more sensitive to the system model parameters. In [29], a duty cycle model predictive direct power control

method is proposed, which uses double vectors to control in two control intervals and uses redundant switching states to control midpoint potential fluctuations, reducing current harmonic content and improving the steady-state performance of the Vienna rectifier. However, there are some problems such as on-line optimization difficulty, high sampling frequency and low system stability, which make it difficult to apply in practice. In [30], a passive current auto-disturbance rejection control algorithm with nonlinear virtual damping injection was proposed to improve the power factor and anti-disturbance performance of the Vienna rectifier, but the control of the midpoint potential was not considered. In [31], repetitive control was combined with PI control to enhance the ability of harmonic suppression, but the anti-disturbance is poor. Literature [32] proposed a new type of topology, using particle swarm optimization algorithm to optimize the gain parameters of the switch, improve the voltage gain of the converter, improve the power factor, and reduce the total harmonic distortion. However, the calculation amount of the algorithm is large, and the system response time is long. Literature [33] optimizes from the topological structure and modulation mode, and realizes zero-voltage switching. Literature [34] combines resonance control with sliding mode control, and proposes a general control strategy suitable for different situations, which improves the power tracking performance. In reference to the problem of resonance, the literature [35] injected a sinusoidal harmonic voltage whose amplitude is related to the power factor into the sinusoidal reference voltage, and designed an LCL filter to reduce the resonance current and improve the current quality.

The above studies have not considered the situation that the Vienna rectifier is affected by external interference in actual work and the internal components are affected by the environment and the parameter changes. In view of this, this paper constructs an improved power mathematical model that includes the total uncertainty of the system, and proposes a hybrid control strategy that combines direct power control and sliding mode control. Firstly, aiming at the chattering problem in sliding mode control, a new type of reaching law was designed and compared with the traditional reaching law. In order to improve the anti-disturbance of the system, the RBF neural network is used to estimate and compensate the uncertain part of the system. Secondly, in view of the distortion of the AC current measured at the zero crossing, the cause of the distortion was studied, and a reactive power compensation scheme was proposed. Space vector modulation (SVPWM) is used to generate trigger signal. The system robustness is improved and the current zero crossing distortion is effectively improved. Finally, the effectiveness of the proposed method is verified by Matlab/simulink simulation and a 5kW physical platform.

II. VIENNA RECTIFIER POWER MODEL WITH UNCERTAIN

The topological structure of the three-level T-type Vienna rectifier is shown in Figure 1. e_a, e_b, and e_c are three-phase AC voltage sources, L is the input side filter inductance, R is the input side equivalent resistance, and the rectifier bridge consists of 6 fast recovery diodes. constitute. S_a, S_b, S_c are two-way power switches connected to the neutral point of the DC side. Each two-way power switch is composed of 2 MOSFET switch tubes and two diodes. C_1 and C_2 are DC side filter capacitors, and R_L is the load.

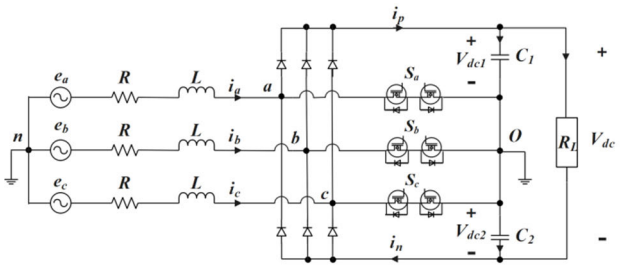

FIGURE 1. Topology of the three-phase Vienna rectifier.

According to the theory of instantaneous power, the complex power of the Vienna rectifier when the three-phase grid voltage is balanced is:

$$S = P + jQ = e^{j\omega t} e_{dq} \overline{e^{j\omega t} i_{dq}}$$

where $e_{dq} = e_d + \mathrm{j}e_q$, $i_{dq} = i_d + ji_q$, "——" is a conjugate complex number.

Instantaneous power differential Equation:

$$\frac{d}{dt}\begin{bmatrix} P \\ Q \end{bmatrix} = \frac{d}{dt}\begin{bmatrix} e_d & e_q \\ e_q & -e_d \end{bmatrix}\begin{bmatrix} i_d \\ i_q \end{bmatrix} + \begin{bmatrix} e_d & e_q \\ e_q & -e_d \end{bmatrix} \times \frac{d}{dt}\begin{bmatrix} i_d \\ i_q \end{bmatrix} \quad (1)$$

The state equation of active power and reactive power and the square of the output voltage can be expressed in the following form:

$$\begin{cases} \dfrac{d({V_{dc}}^2)}{dt} = -\dfrac{4}{R_L C}{V_{dc}}^2 + \dfrac{4}{C}P \\ \dfrac{dP}{dt} = -\dfrac{R}{L}P + \dfrac{1}{L}\left(\dfrac{3}{2}{e_d}^2 - L\omega Q - \dfrac{3}{2}e_d V_d\right) \\ \dfrac{dQ}{dt} = -\dfrac{R}{L}Q + \dfrac{1}{L}\left(L\omega P - \dfrac{3}{2}e_d V_q\right) \end{cases} \quad (2)$$

where, V_{dc} is the output voltage; P is the active power; Q is the reactive power; e_d, e_q are the components of the three-phase AC voltage in the dq rotating coordinate system.

$$V_d = S_{dp}V_{dc1} - S_{dn}V_{dc2},\ V_q = S_{qp}V_{dc1} - S_{qn}V_{dc2}$$

In the actual operation process, the Vienna rectifier will be affected by many internal or external disturbances, for example, temperature changes, vibrations change the parameters of inductance L and resistance R; disturbances caused by load changes. However, the disturbance factor is not considered in Equation (1), so it is difficult to maintain the stable operation of the rectifier when it is disturbed. Therefore, a power control model of the Vienna rectifier considering the uncertainty of

the system is established:

$$\begin{cases} \dfrac{dP}{dt} = -\dfrac{\hat{R}}{\hat{L}}P + \dfrac{1}{\hat{L}}\left(\dfrac{3}{2}e_d^2 - \hat{L}\omega Q - \dfrac{3}{2}e_d V_d\right) + G_p \\ \dfrac{dQ}{dt} = -\dfrac{\hat{R}}{\hat{L}}Q + \dfrac{1}{\hat{L}}\left(\hat{L}\omega P - \dfrac{3}{2}e_d V_q\right) + G_q \end{cases} \tag{3}$$

Since the true values of the parameters L and R in the equation are uncertain terms, the nominal setting values of the parameters L and R are respectively $\hat{L}$ and $\hat{R}$, and the error terms are $\tilde{L}$ and $\tilde{R}(L = \hat{L} + \tilde{L}, R = \hat{R} + \tilde{R})$. G_p and G_q respectively represent the total uncertainty or total interference including parameter uncertainties and external disturbances in the active power and reactive power models. Suppose there is an upper limit δ_p, δ_q, that is $|G_p| < \delta_p$, $|G_q| < \delta_q$, $\delta_p, \delta_q > 0$.

III. SLIDING MODE DIRECT POWER CONTROL WITH REACTIVE POWER COMPENSATION

A. DESIGN OF NEW SLIDING MODE REACHING LAW

Sliding mode variable structure control is widely used in nonlinear system control, but it has the problem of "chattering", which reduces the control effect. In order to improve the chattering problem and increase the response speed of the system, this section will introduce a new type of reaching law. At the same time, aiming at the uncertain part of the system model, the RBF neural network is used to estimate and compensate the uncertain model of the system. The reason for the distortion of the AC side current at the zero crossing is analyzed, and the method of compensating reactive power is proposed to optimize the solution.

In order to improve the response speed of the system and reduce chattering, a new approaching law is designed:

$$\xi = \begin{cases} -k_1 |S|^{\varepsilon_1} \operatorname{sgn}(S) - k_2 e^{\varepsilon_2 |S|} \operatorname{sgn}(S) \\ \qquad |S| > set \\ -\mu \left(k_3 + e^{-\varepsilon_3 |S|}\right)^{-1} \operatorname{sgn}(S) - k_4 |S| \tanh(S) \\ \qquad |S| < set \end{cases} \tag{4}$$

where k1>0, k2>0, k3>0, k4>0, $0<\varepsilon_1<1$, $1<\varepsilon_2$, $0<\varepsilon_3<1$, $\mu>0$. When the system is far away from the sliding surface, that is $|S| \gg set$, $-k_2 e^{\varepsilon_2 |S|}\operatorname{sgn}(S)$ plays a leading role, making the system quickly approach the sliding surface, when $|S|$ is close to set $-k_1|S|^{\varepsilon_1}\operatorname{sgn}(S)$ plays a leading role, avoiding the problem of slow convergence when $|S| > 1$. Compared with the traditional approaching law, it can approach the sliding surface at a faster speed. When $|S| \leq set$, $-k_4|S|\tanh(S)$ plays a leading role, reducing the approach speed while approaching the sliding surface, ensuring the smooth convergence of the system, $\mu(k_3 + e^{-\varepsilon_3|S|})^{-1}\operatorname{sgn}(S)$ is to make the system slowly decrease to a fixed value at the specified speed when it is close to the sliding surface. Reasonably setting a fixed minimum value can control the amplitude of chattering, ensure the robustness of the system, and also make up for the slow convergence speed of the system near the sliding mode surface.

In order to verify the effectiveness of the proposed new approaching law, we compared it with the traditional constant velocity approaching law, double power approaching law, and no additional item approaching law. The results are shown in Figure 2. It can be seen that in the approaching stage, compared with the traditional method, the method proposed in this paper can approach the sliding surface more quickly, and when it is close to the sliding surface, it converges gently and then reaches the sliding surface and starts sliding movement. The approach speed is improved and chattering is reduced. When there are no additional items, the continuous attenuation of the system close to the sliding mode surface results in the system's delay in reaching the sliding mode surface, resulting in an increase in system response time. The validity of the proposed law of reaching is verified.

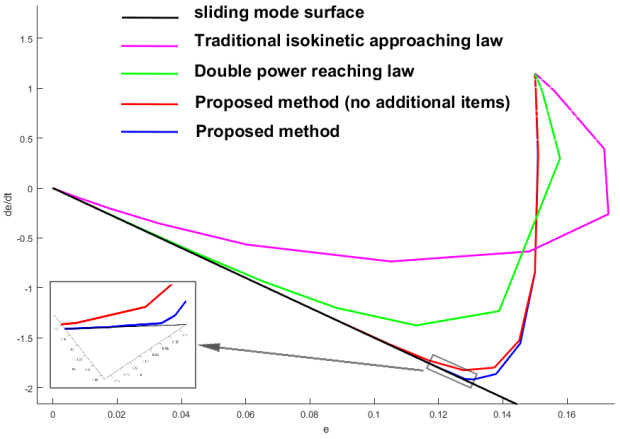

FIGURE 2. Comparison chart of the proposed approaching law and the traditional approaching law approximation effect.

B. CONTROL LAW DESIGN

In order to make the active power track the reference active power P_{ref} stably and the reactive power stably track the reference reactive power Q_{ref}, the following sliding mode surface is designed:

$$\begin{cases} S_1 = P_{ref} - P \\ S_2 = Q_{ref} - Q \end{cases} \tag{5}$$

Combining equations (3) (4) (5) can be obtained:

$$\begin{cases} \dot{P}_{ref} + \dfrac{\hat{R}}{\hat{L}}P + \dfrac{1}{\hat{L}}\left(\dfrac{3}{2}e_d^2 - \hat{L}\omega Q - \dfrac{3}{2}e_d V_d\right) + G_p = \xi_p \\ \dot{Q}_{ref} + \dfrac{\hat{R}}{\hat{L}}Q + \dfrac{1}{\hat{L}}\left(\hat{L}\omega P - \dfrac{3}{2}e_d V_q\right) + G_q = \xi_q \end{cases} \tag{6}$$

where Gp and Gq are the total uncertainty of the system, which is estimated and compensated by the radial basis function neural network:

$$h_j = \exp\left(\frac{\|X - c_j\|^2}{2b_j^2}\right)$$

$$f = W^T h(X) + \varepsilon$$

where, X is the network input; j is the JTH node in the hidden layer of the network; $h = [h_j]^T$ is the gaussian basis function

output of the network, W is the ideal weight of the network; ε is the approximation error of the network, $\varepsilon \leq \varepsilon_N$; f is the network output.

The input of the neural network is $X = [x_1\ x_2]^{\mathrm{T}}$, then the output of the neural network is:

$$\hat{f}(x) = \hat{W}^T h(X)$$

In this paper, the output of the above neural network is used to fit the total uncertainty G of the system, and the ideal weight vector W is known to exist so that:

$$G = W^T h(X) + \varepsilon$$

where, $X = [S_1\ S_2]^{\mathrm{T}}$, since W is unknown, $\hat{W}$ is assumed to be the estimated value of W, so the total disturbance estimator $\hat{G} = \hat{W}^T h(x)$ can be obtained. In summary, the control law can be designed:

$$\begin{cases} V_d = \dfrac{2\hat{L}}{3e_d}\left(-\dot{P}_{ref} - \dfrac{\hat{R}}{\hat{L}}P + \dfrac{3e_d^2}{2\hat{L}} - \omega Q + \hat{G}_p\right) + \xi_p \\ V_q = \dfrac{2\hat{L}}{3e_d}\left(-\dot{Q}_{ref} - \dfrac{\hat{R}}{\hat{L}}Q + \omega Q + \hat{G}_q\right) + \xi_q \end{cases} \tag{7}$$

Stability proof:

Combining equations (3) and (7) can be obtained:

$$\begin{aligned} \dot{S}_1 &= G_d - \hat{G}_d + \xi_p \\ &= W^T h(X) + \varepsilon - \hat{W}^T h(X) + \xi_p \\ &= \tilde{W}^T h(X) + \varepsilon + \xi_p \end{aligned} \tag{8}$$

where, $\tilde{W} = W^* - \hat{W}$

Design the adaptive law of radial basis neural network:

$$\dot{\hat{W}} = \frac{1}{\eta} \cdot S_1 h(x) \tag{9}$$

Design the Lyapunov function:

$$V = \frac{1}{2}S_1^2 + \frac{1}{2}\eta \tilde{W}^T \tilde{W} \tag{10}$$

where, $\eta > 0$

Take the derivative of Equation (10):

$$\dot{V} = S_1 \cdot \dot{S}_1 + \eta \tilde{W}^T \dot{\tilde{W}} \tag{11}$$

Substitute Equation (8) and (9) into Equation (11) to obtain:

$$\begin{aligned} \dot{V} &= S_1 \cdot \dot{S}_1 + \eta \tilde{W}^T \dot{\tilde{W}} \\ &= S_1 \cdot \tilde{W}^T h(X) + S_1(\varepsilon + \xi_p) - \eta \tilde{W}^T \dot{\hat{W}} \\ &= \tilde{W}^T \left(S_1 h(X) - \eta \dot{\hat{W}}\right) + S_1(\varepsilon + \xi_p) \\ &= S_1(\varepsilon + \xi_p) \end{aligned} \tag{12}$$

When $|S_1|>$set:

$$\begin{aligned} \dot{V} &= S_1\varepsilon - k_1 |S|^{\varepsilon_1} S_1 \mathrm{sgn}(S) \\ &\quad -k_2 e^{\varepsilon_2 |S|} S_1 \mathrm{sgn}(S) \\ &= S_1\varepsilon - k_1 |S|^{\varepsilon_1 + 1} - k_2 e^{\varepsilon_2 |S|} |S_1| \end{aligned} \tag{13}$$

When |S1|<set:

$$\begin{aligned} \dot{V} &= S_1\varepsilon - \mu \left(k_3 + e^{-\varepsilon_3 |S|}\right)^{-1} S_1 \mathrm{sgn}(S) \\ &\quad -k_4 |S| S_1 \tanh(S) \\ &= S_1\varepsilon - \mu \left(k_3 + e^{-\varepsilon_3 |S|}\right)^{-1} |S_1| - k_4 |S| S_1 \tanh(S) \end{aligned} \tag{14}$$

Because $\varepsilon \ll k_1, k_2, k_3, k_4$, so $\dot{V} \leq 0$, and because $V \geq 0$, we can prove that S_1 is bounded. When $\dot{V} \equiv 0$, $S_1 = 0$, so the system is asymptotically stable. In the same way, it can be proved that S_2 is bounded and asymptotically stable.

C. THE CAUSE OF CURRENT ZERO-CROSSING DISTORTION AND ITS COMPENSATION METHOD

Fig. 3 is the vector diagram when the d-axis in the rotating coordinate system is rotated to the B-phase zero crossing point. It can be seen from Fig. 3(a) that the inductance voltage $\mathrm{V_L}$ causes the reference voltage $\mathrm{V_T}$ to lag the current vector i, so the sign changes from negative to positive when the current i crosses zero through phase B, while the sign of the reference voltage $\mathrm{V_T}$ remains negative until it continues to rotate θ Angle. In this process, the trigger signal of the B-phase bidirectional diode will produce the opposite trigger signal, resulting in zero-crossing distortion of the B-phase current. Similarly, the A-phase current and the B-phase current will also produce current distortion, which reduces the current quality. Therefore, an optimization measure for reactive power compensation is proposed. As shown in Fig. 3(b), the phase angle θ between the current i and the reference voltage $\mathrm{V_T}$ is eliminated by the compensation current i_{qc}.

Compensated reactive power Q:

$$\begin{aligned} Q_c &= -\frac{3}{2}e_d i_{qc} = \frac{3}{2}e_d i_d \tan\theta \\ &= \frac{3}{2}e_d i_d \frac{V_L}{e_d} \\ &= \frac{3}{2}e_d i_d \frac{\omega L_S i_d}{e_d} \\ &= 1.5\omega L i_d^2 \end{aligned} \tag{15}$$

Compensated reactive power reference value Q_{ref}:

$$Q_{ref} = Q_c = 1.5\omega L i_d^2 \tag{16}$$

The block diagram of the proposed improved sliding mode direct power control strategy control system with reactive power compensation is shown in Fig. 4. The three-phase input voltage and current are transformed into components e_{d}, e_{q}, i_{d} and i_{q} in the dq rotating coordinate system through coordinate transformation. According to the instantaneous power theory, the active power P and the reactive power Q are obtained. The reference value Pref of active power P is calculated by the outer loop control, and the reference value Qref of reactive power Q is calculated by the reactive power compensator. The RBF neural network calculated the total disturbance of the system, and input the above parameters to the improved sliding mode direct power controller in Eq. (7), the decoupled

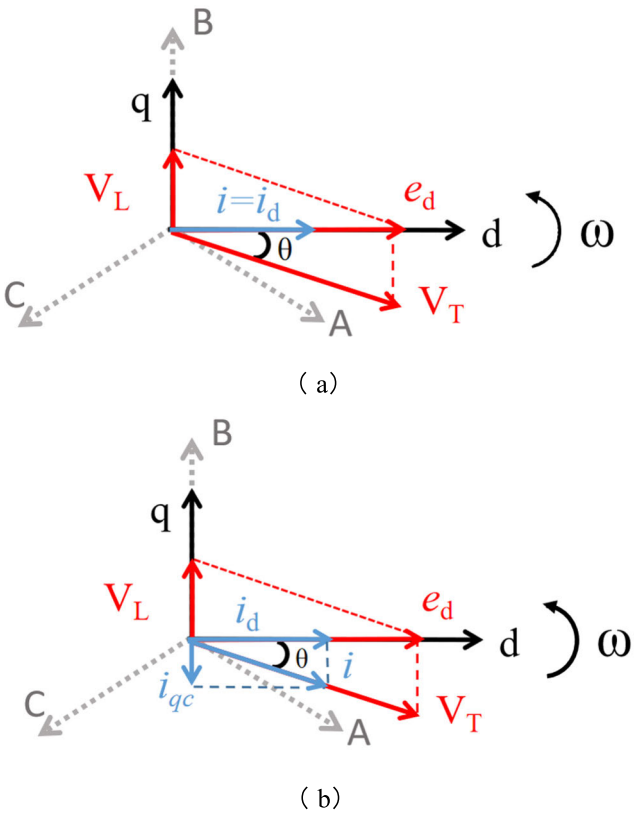

FIGURE 3. The vector diagram when the d-axis in the rotating coordinate system is rotated to the zero-crossing point of phase B.

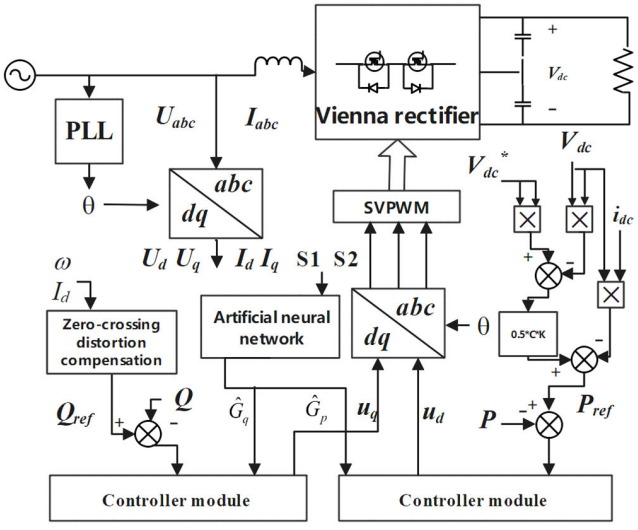

FIGURE 4. Improved sliding mode direct power control strategy control system with reactive power compensation block diagram.

control variables u_p and u_q were obtained. Finally, after coordinate transformation, decoupling and SVPWM modulation, the final switching signals S_a, S_b, and S_c are obtained.

IV. SIMULATION RESULTS

In order to verify the effectiveness of the proposed method, Matlab/Simulink is used to carry out simulation experiments. The proposed method is compared with the hybrid control

TABLE 1. Simulation parameters of the Vienna rectifier.

PARAMETER	Value
AC grid voltage	e_a=e_b=e_c=110V
Grid frequency	50Hz
Filter inductance	2mH
DC-link capacitor	2000μF
Switching frequency	20kHz
DC-link load	54Ω
Output voltage	400V

with PI control in the outer loop and double power approaching sliding mode control in the inner loop. The simulation parameters are shown in Table 1.

The two controller parameters are set as follows:

In PI control, the increase of the proportional coefficient can improve the response speed of the system, but too large a proportional coefficient will cause a large overshoot and even cause the system to be unstable; Increasing the integral coefficient can reduce the steady-state error of the system, but an excessive integral will aggravate the overshoot and even cause oscillation. In the double-power approaching law, if the double-power coefficients k_1 and k_2 are too large, it will aggravate the system chattering, and if the double-power coefficients are too small, the convergence speed of the system will be slower. The double power exponents α_1 and α_2 can adjust the convergence speed of the system far and near the sliding surface. After actual debugging, the parameter settings are as follows: Proportional coefficient KP = 14, integral coefficient KI = 0.55, k_1 = 1200, k_2 = 350, $\alpha_1 = 0.5$, $\alpha_2 = 0.5$.

In the method proposed in this paper, the reaching law coefficients k_1, k_2, and k_4 affect the control accuracy of the system. Increasing the reaching law coefficient will reduce the tracking error of the system, but at the same time it will also increase the chattering. If the coefficient is too large, it will even cause the system to diverge. Decreasing the reaching law coefficient will reduce the control accuracy and speed of the system. If the reaching law index ε_1 and ε_2 are too large, the stability of the system will be reduced, and too small will increase the system error. The parameter ε_3 in the additional item can adjust the change speed of the additional item with the distance S of the sliding surface. Together with the parameters μ and k_3, it controls the fixed value of the approaching speed of the system when it is closer to the sliding surface. After actual debugging, the parameters are set as follows: k_1 = 15.2, k_2 = 4.7, k_3 = 113, k_4 = 45, $\varepsilon_1 = 0.3$, $\varepsilon_2 = 1.4$, $\varepsilon_3 = 0.3$, μ = 1200, $Cj = 5$, $\eta = 0.2$, the radial basis function center is evenly distributed in $[-2,2]$, the width b_j = 20, and the number of hidden layer neurons is 7.

Fig. 5 are the start-up response simulation waveforms of the Vienna rectifier. Fig. 5(a) is the start-up response

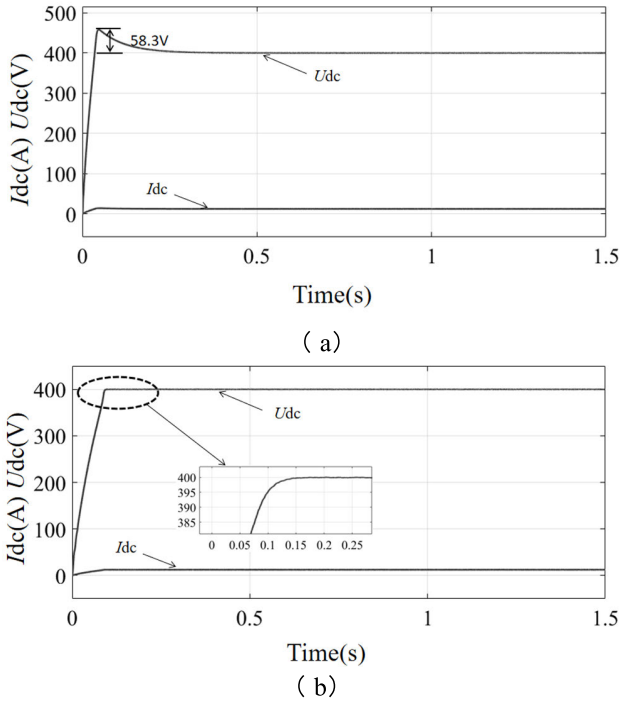

FIGURE 5. The start-up response waveform of the output voltage and current of the Vienna rectifier. (a)traditional hybrid control method, (b)proposed method.

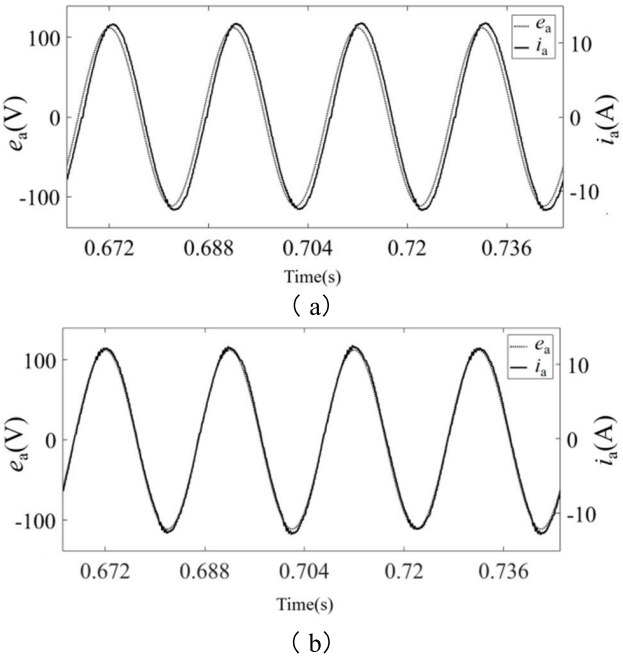

FIGURE 6. The voltage and current simulation waveforms of the Vienna rectifier after stable operation. (a)traditional hybrid control method, (b)proposed method.

simulation waveform under the traditional hybrid control method, and Fig. 5(b) is the start-up response simulation waveform under the proposed control method. The output voltage of the rectifier is set to 400V. It can be seen from the fig. 5(a) that the traditional hybrid control method has voltage overshoot after the system is started. The voltage overshoot

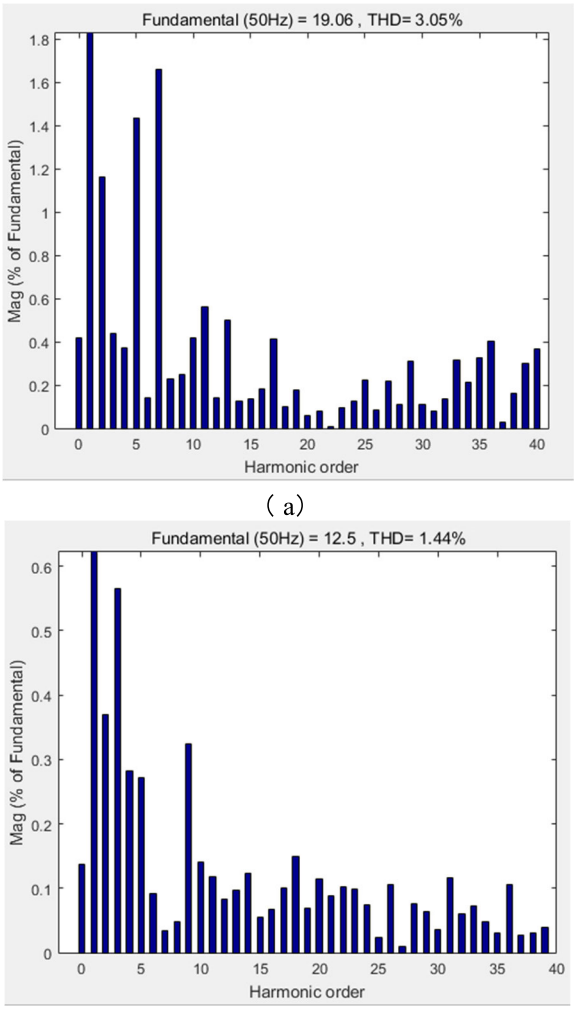

FIGURE 7. Current Total Harmonic Distortion of the Vienna Rectifier. (a)traditional hybrid control method, (b)proposed method.

reaches 58.3V and reaches the steady-state value of 400V after about 371ms. However, It can be seen from the fig. 5(b) that the proposed method has no voltage overshoot, and the steady-state value of 400V is reached after about 185ms. The simulation results show that the proposed method has stronger voltage tracking ability, faster response speed, and shows better startup performance.

Fig. 6 is the voltage and current simulation results after the Vienna rectifier is stable. Fig. 6(a) is the simulation waveform under the traditional hybrid control method, and Fig. 6(b) is the simulation waveform under the proposed method. Fig. 7 is the simulation result of current total harmonic distortion,, Fig. 7(a) is the simulation waveform under the traditional hybrid control method, and Fig. 7(b) is the simulation waveform under the proposed method. It can be seen from Fig. 6(a) and Fig. 7(a) that there is a large phase difference between the voltage and current in the traditional hybrid control, and the current has obvious distortion at the zero-crossing point, and the current total harmonic distortion is 3.05%. It can be seen from Figure 6(b) and Figure 7(b) that the voltage and

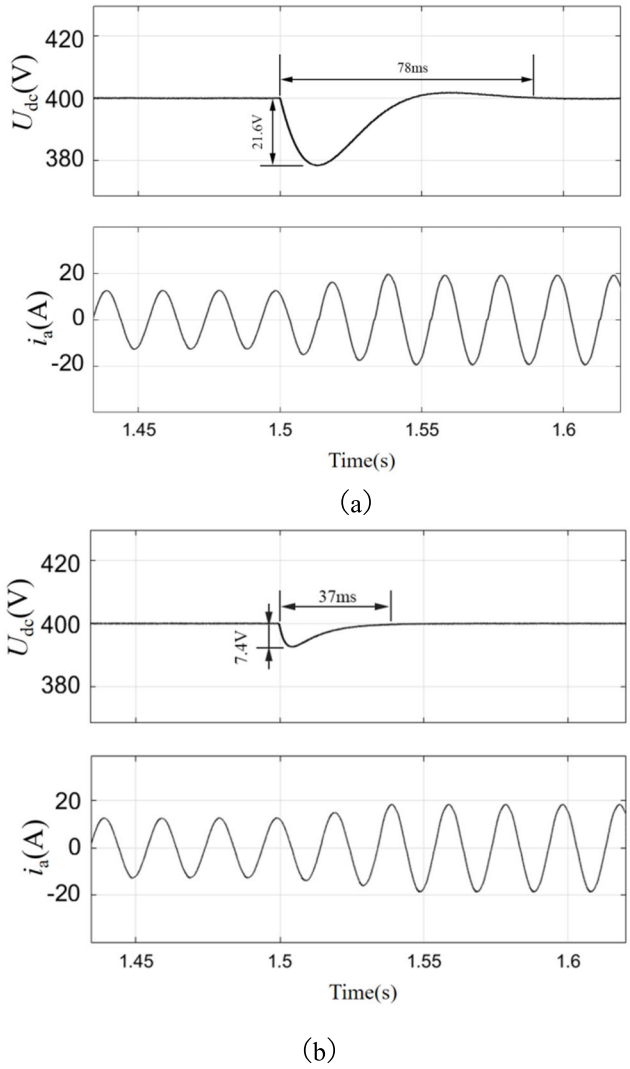

FIGURE 8. Simulation results of Vienna rectifier changing load. (a)traditional hybrid control method, (b)proposed method.

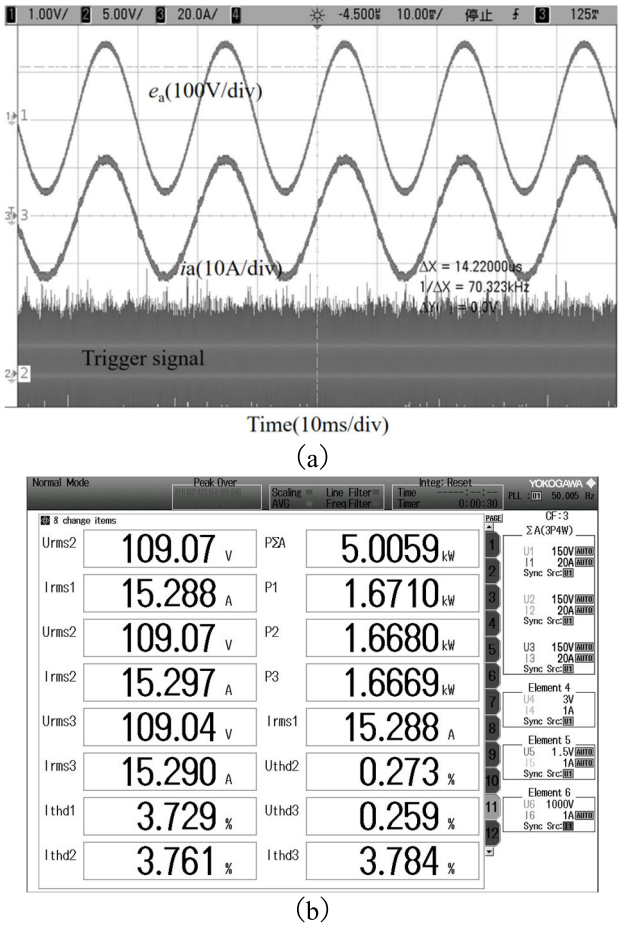

FIGURE 9. The voltage and current experimental waveforms and waveform quality of the Vienna rectifier under the traditional hybrid control method. (a)voltage and current experimental waveforms, (b)voltage and current waveform quality.

current of the proposed method can maintain the same phase to ensure the unit power operation of the Vienna rectifier. The quality of the voltage and current waveform has been significantly improved and the harmonic distortion of the current at the zero crossing is effectively controlled, and the total harmonic distortion of the current is reduced to 1.44%. The simulation results show that the proposed method has good phase compensation and improved current zero-crossing harmonic distortion performance.

Fig. 8 shows the simulation results of the Vienna rectifier changing the load. Fig. 8(a) shows the simulation results under the traditional hybrid control method, and Fig. 8(b) shows the simulation results under the proposed control method. The load is increased after the Vienna rectifier runs stably for 1.5s. The DC bus voltage of the traditional hybrid control method dropped by 21.6V and returned to the steady-state value after about 78ms. However, the DC bus voltage of the proposed method dropped 7.4V and returned to the steady-state value after about 37ms. The simulation results show that the proposed method has a smaller voltage drop when the load changes, a faster system adjustment speed, and a stronger ability to resist load disturbances.

V. EXPERIMENTAL RESULT

In order to verify the control effect of the control strategy proposed in this paper, a three-phase Vienna rectifier 5kW experimental prototype was built. The DSP chip is TMS320F28021, the switching device MOSFET is SPW47N60C3, and the diode is RHRG30120. The three-phase grid voltage is provided by a 9kVA voltage regulator. The parameters used in the experiment are consistent with those in the simulation.

In order to verify the improvement effect of the proposed method on the input and output performance of the Vienna rectifier, a steady-state experiment was carried out and compared with the traditional hybrid control method. The experimental results are shown in Fig. 9 and Fig. 10. Fig. 9(a) and Fig. 9(b) respectively show the voltage and current waveform and waveform quality under traditional hybrid control method. Fig. 10(a) and Fig. 10(b) respectively show the voltage and current waveform and waveform quality under the proposed control method.

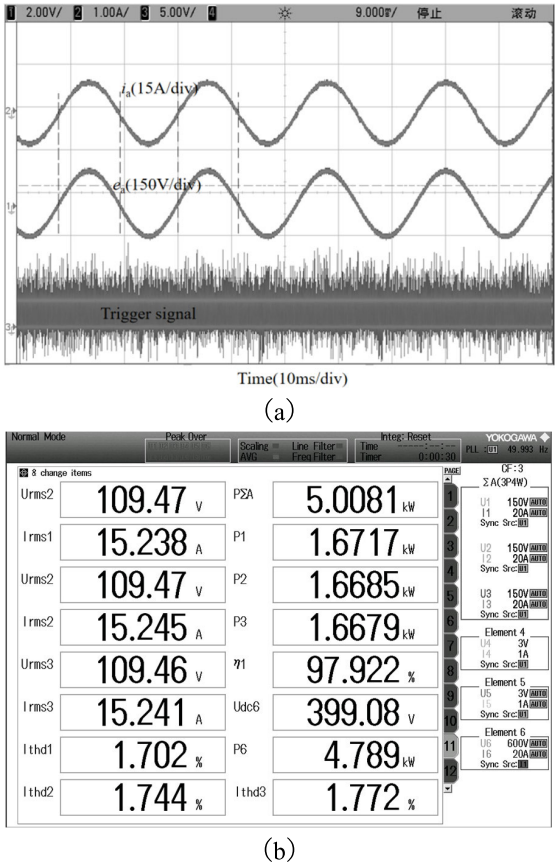

FIGURE 10. The voltage and current experimental waveforms and waveform quality of the Vienna rectifier under the proposed control method. (a)voltage and current experimental waveforms, (b)voltage and current waveform quality.

From Fig. 9(a) and Fig. 10(a), it can be seen that there is a phase difference between the AC voltage and current in the traditional hybrid control method, and the quality of the AC current waveform is poor, and there is a zero-crossing distortion phenomenon. In the proposed method, the AC voltage and current are in the same phase and the voltage and current waveforms show a good sinusoidal shape. It can be seen from Fig. 9(b) and Fig. 10(b) that the total harmonic distortion of the three-phase AC current in the traditional hybrid control method are 3.729%, 3.761%, and 3.784%. In the proposed method, the total harmonic distortion of the three-phase AC current are 1.702%, 1.744%, and 1.772%. The experimental results show that the proposed method has better current quality.

In order to verify the anti-load disturbance capability of the proposed method, a varying load experiment was carried out on the Vienna rectifier. The experimental results are shown in Fig. 11. It can be seen from Fig. 11(a) that in the traditional hybrid control method, the DC bus voltage dropped 11.2V, and the steady state was restored after about 45ms. It can be seen from Fig. 11(b) that in the proposed method, the DC bus voltage drops 4.3V and returns to a steady state after about 25ms. The experimental results show that compared with the traditional method, the proposed method has stronger anti-load disturbance ability.

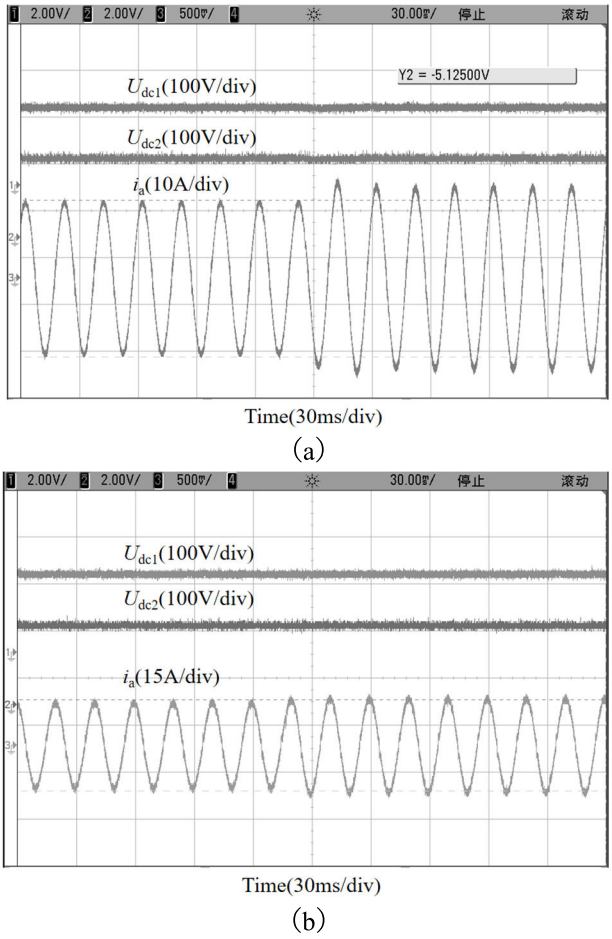

FIGURE 11. Experimental results of Vienna rectifier varying load. (a)traditional hybrid control method, (b)proposed method.

VI. CONCLUSION

In this paper, the uncertainty model of the Vienna rectifier is established, and a new sliding mode direct power control strategy based on neural network is proposed. Estimating and compensating the uncertain model part of the system through a neural network improves the robustness of the rectifier; Improve the system convergence speed and reduce chattering by designing a new approaching law; Through the method of reactive power compensation, the problem of different phases of voltage and current and the problem of current zero-crossing distortion are overcome, the current quality is improved, and the current total harmonic distortion is controlled below 2%; Overcome the voltage overshoot problem in traditional control methods, and the effectiveness of the proposed strategy is verified by simulation and experiment.

REFERENCES

[1] *Moldovan Parliament Declares State of Emergency Over Energy Crisis*, Interfax, Russia & CIS Energy Newswire, Moscow, Russia, 2021.
[2] *Novak: European Energy Crisis Stems From Pressure of Transition From Traditional Energy Sources*, Interfax, Russia & CIS Energy Newswire, Moscow, Russia, 2021.
[3] H. Chen, H. Ling, and Y. Xu, "Physical energy storage technology in the energy revolution," *Bull. Chin. Acad. Sci.*, vol. 34, no. 4, pp. 450–459, 2019.

[4] J. Hu, K. Wang, X. Ai, X. Han, G. Yang, and X. Yusheng, "Interactive energy: Transactive energy: An effective mechanism for balancing electric energy system," *Proc. CSEE*, vol. 39, no. 4, pp. 953–965, 2019.
[5] Z. Qingyan, *Research on Vienna Rectifier Control Method*. Hefei, China: Hefei Univ. Technology, 2021.
[6] J.-S. Lee, K.-B. Lee, and F. Blaabjerg, "Predictive control with discrete space-vector modulation of Vienna rectifier for driving PMSG of wind turbine systems," *IEEE Trans. Power Electron.*, vol. 34, no. 12, pp. 12368–12383, Dec. 2019.
[7] A. R. Izadinia and H. R. Karshenas, "Current shaping in a hybrid 12-pulse rectifier using a Vienna rectifier," *IEEE Trans. Power Electron.*, vol. 33, no. 2, pp. 1135–1142, Feb. 2018.
[8] W. Ding, C. Zhang, F. Gao, B. Duan, and H. Qiu, "A zero-sequence component injection modulation method with compensation for current harmonic mitigation of a Vienna rectifier," *IEEE Trans. Power. Electron.*, vol. 34, no. 1, pp. 801–814, Jan. 2019.
[9] A. Rajaei, M. Mohamadian, and M. Dems, "Vienna-rectifier-based direct torque control of PMSG for wind energy application," *IEEE Trans. Ind. Electron.*, vol. 60, no. 7, pp. 2919–2929, 2013.
[10] M. Luqman, G. Yao, L. Zhou, and A. Lamichhane, "Analysis of variable speed wind energy conversion system with PMSG and Vienna rectifier," in *Proc. 14th IEEE Conf. Ind. Electron. Appl. (ICIEA)*, Jun. 2019, pp. 1296–1301.
[11] R. Pandey and B. Singh, "An electric vehicle charger based on Vienna rectifier and resonant LLC converter," in *Proc. IEEE Int. Conf. Power Electron., Drives Energy Syst. (PEDES)*, Dec. 2020, pp. 1–6.
[12] M. V. Gogate, H. M. Suryawanshi, P. P. Nachankar, V. V. P. Reddy, L. N. Chintalapudi, and G. Devasuth, "Comparative analysis for semiconductor device selection in Vienna rectifier for fast EV charging application," in *Proc. IEEE 1st Int. Conf. Smart Technol. Power, Energy Control (STPEC)*, Sep. 2020, pp. 1–6.
[13] L. Ping, W. Jiuhe, and Z. Qinghe, "Hybrid variable-frequency SVPWM strategy for current harmonics suppression of Vienna rectifier," *High Voltage Eng.*, vol. 22, no. 9, pp. 1–12, 2021.
[14] T. Wang *et al.*, "An improved space-vector modulation for Vienna rectifier to eliminating current distortion around zero-crossing point," *Trans. China Electrotech. Soc.*, vol. 34, no. 18, pp. 3854–3864, 2019.
[15] H. Xu, W. Yao, and S. Shao, "Improved SVPWM schemes for Vienna rectifiers without current distortion," in *Proc. IEEE Energy Convers. Congr. Expo. (ECCE)*, Oct. 2017, pp. 3410–3414.
[16] X. Wang, R. Shao, and Y. Li, "Research on control strategy of VIENNA rectifier based on sliding mode variable structure and IMC," *Appl. Electron. Technique*, vol. 44, no. 9, pp. 150–153, 2018.
[17] M. Hui, Y. Shengyang, W. Shuzheng, and W. Wei, "Research on QPR and sliding-mode control strategy for three-phase Vienna rectifier," *Appl. Electron. Techn.*, vol. 45, no. 1, pp. 118–121, 2019.
[18] W.-Z. Song, F. X. Xing, H. Yan, L. Empringham, L. D. Lillo, P. Wheeler, J. Li, and Y. R. Zhong, "A hybrid control method to suppress the three-time fundamental frequency neutral-point voltage fluctuation in a VIENNA rectifier," *IEEE J. Emerg. Sel. Topics Power Electron.*, vol. 4, no. 2, pp. 468–480, Jun. 2016.
[19] M. H. Islam and M. A. Razzak, "Design of a modified Vienna rectifier for power factor correction under different three phase loads," in *Proc. 5th Int. Conf. Informat., Electron. Vis. (ICIEV)*, May 2016, pp. 764–770.
[20] G. Rajendran, C. A. Vaithilingam, N. Misron, K. Naidu, and M. R. Ahmed, "Voltage oriented controller based Vienna rectifier for electric vehicle charging stations," *IEEE Access*, vol. 9, pp. 50798–50809, 2021.
[21] Z. Qingyan and W. Peidong, "Modulation method for reducing current zero-CrossingDistortion of Vienna rectifier," *Elect. Energy Manage. Technol.*, vol. 2, pp. 81–87, Feb. 2021.
[22] Z. Wang, A. Zhang, and H. Zhang, "Research on voltage sliding mode control of Vienna rectifier," in *Proc. Chin. Control Decis. Conf. (CCDC)*, Aug. 2020, pp. 251–255.
[23] Y. Sun, G. Gao, and S. Wang, "Research on sliding mode control strategy of Vienna rectifier in front stage of high stability magnet power supply," in *Proc. 7th Int. Conf. Inf. Sci. Control Eng. (ICISCE)*, Dec. 2020, pp. 2130–2135.
[24] Y. Yao, X. Huang, G. Chen, K. Xing, and D. Ma, "Research on VIENNA rectifier based on active disturbance rejection control," in *Proc. 13th IEEE Conf. Ind. Electron. Appl. (ICIEA)*, May 2018, pp. 299–304.
[25] J. Li, M. Wang, J. Wang, Y. Zhang, D. Yang, J. Wang, and Y. Zhao, "Passivity-based control with active disturbance rejection control of Vienna rectifier under unbalanced grid conditions," *IEEE Access*, vol. 8, pp. 76082–76092, 2020.
[26] W. Song, "Hybrid control method to suppress neutral-point voltage fluctuation for three-phase three-level VIENNA rectifier," *High Power Laser Part. Beams*, vol. 31, no. 4, 2019, Art. no. 040016.
[27] X. Feng, Y. Tao, X. Cui, K. Shao, and Y. Wang, "Sliding mode and predictive current control strategy of the three-phase Vienna rectifier," *J. Power Electron.*, vol. 20, no. 3, pp. 743–753, May 2020.
[28] W. Zhu, C. Chen, and S. Duan, "A model predictive control method with discrete space vector modulation of Vienna rectifier," *Proc. CSEE*, vol. 39, no. 20, pp. 6008–6016 and 6181, 2019.
[29] Z. Zuo, W. Yang, and L. Zhengming, "Predictive control strategy of Vienna rectifier model based on duty cycle control," *Power Syst. Protection Control*, vol. 49, no. 10, pp. 162–169, 2018.
[30] W. Xiandong, S. Ruping, and Y. Yan, "Research on control strategy of Vienna rectifier based on passivity-based and active disturbance rejection controller," *Power Syst. Technol.*, vol. 27, no. 8, pp. 1–12, 2021.
[31] C. Zheng, "Repetitive control realization of Vienna rectifier," *Power Electron.*, vol. 55, no. 7, pp. 35–38, 2021.
[32] R. Brindha, A. A. Christy, R. Elanthirayan, and R. Krishnamoorthy, "A modified inductor and control models of three phase Vienna rectifier topology using particle swarm optimization algorithm," *J. Ambient Intell. Humanized Comput.*, vol. 12, no. 6, pp. 6107–6116, Jun. 2021.
[33] S. Zhao, U. Borovic, M. Silva, O. García, J. A. Oliver, P. Alou, J. A. Cobos, and P. Pejovic, "Modified Vienna rectifier III to achieve ZVS in all transitions: Analysis, design and validation," *IEEE Trans. Power Electron.*, vol. 36, no. 12, pp. 13404–13422, May 2021.
[34] Y. Zhou, A. Zhang, H. Zhang, J. Huang, W. Yang, and L. Zhang, "Proportional integral resonance based sliding mode control of Vienna rectifier for charging station of tramcar under unbalanced power supply," *Int. Trans. Electr. Energy Syst.*, vol. 30, no. 10, Oct. 2020, Art. no. e12518.
[35] J. H. Park, J. S. Lee, and K. B. Lee, "Sinusoidal harmonic voltage injection PWM method for Vienna rectifier with an LCL-filter," *IEEE Trans. Power Electron.*, vol. 36, no. 3, pp. 2875–2888, Mar. 2021.

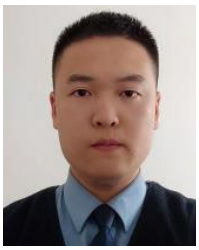

YAODONG WANG was born in Xi'an, China, in 1997. He received the bachelor's degree in electrical engineering and automation from Air Force Engineering University, in 2020, where he is currently pursuing the master's degree. His research interests include rectifier control, nonlinear control, and intelligent algorithms.

YINGHUI LI was born in Hunan, China, in 1966. She is currently a Professor with Air Force Engineering University. She is a Doctoral and Postdoctoral Supervisor with Xi'an Jiaotong University. She is a Control Science and Engineering Expert and has been engaged in academic research on advanced control theory and applications.

SHUN HUANG was born in Wuhan, China, in 1997. He received the bachelor's degree in electrical engineering and automation from the Nanjing University of Aeronautics and Astronautics, in 2020. He is currently pursuing the master's degree. His research interests include rectifier control, nonlinear control, and motor design.